Hyperfine interactions and internal rotation in methanol

Boy Lankhaar

Theoretical Chemistry, Institute for Molecules and Materials, Radboud University Heyendaalseweg 135, 6525 AJ Nijmegen, The Netherlands
and
Onsala Space Observatory, Chalmers University of Technology, 439 92 Onsala, Sweden

Gerrit C. Groenenboom

Theoretical Chemistry, Institute for Molecules and Materials, Radboud University Heyendaalseweg 135, 6525 AJ Nijmegen, The Netherlands

Ad van der Avoird*

Theoretical Chemistry, Institute for Molecules and Materials, Radboud University Heyendaalseweg 135, 6525 AJ Nijmegen, The Netherlands

Supplementary material

* Electronic address: A.vanderAvoird@theochem.ru.nl

OTHER SPECTRA ANALYZED

Figures 1 to 7 in this supplement show hyperfine structure resolved spectra for different rotational transitions that were also analyzed.

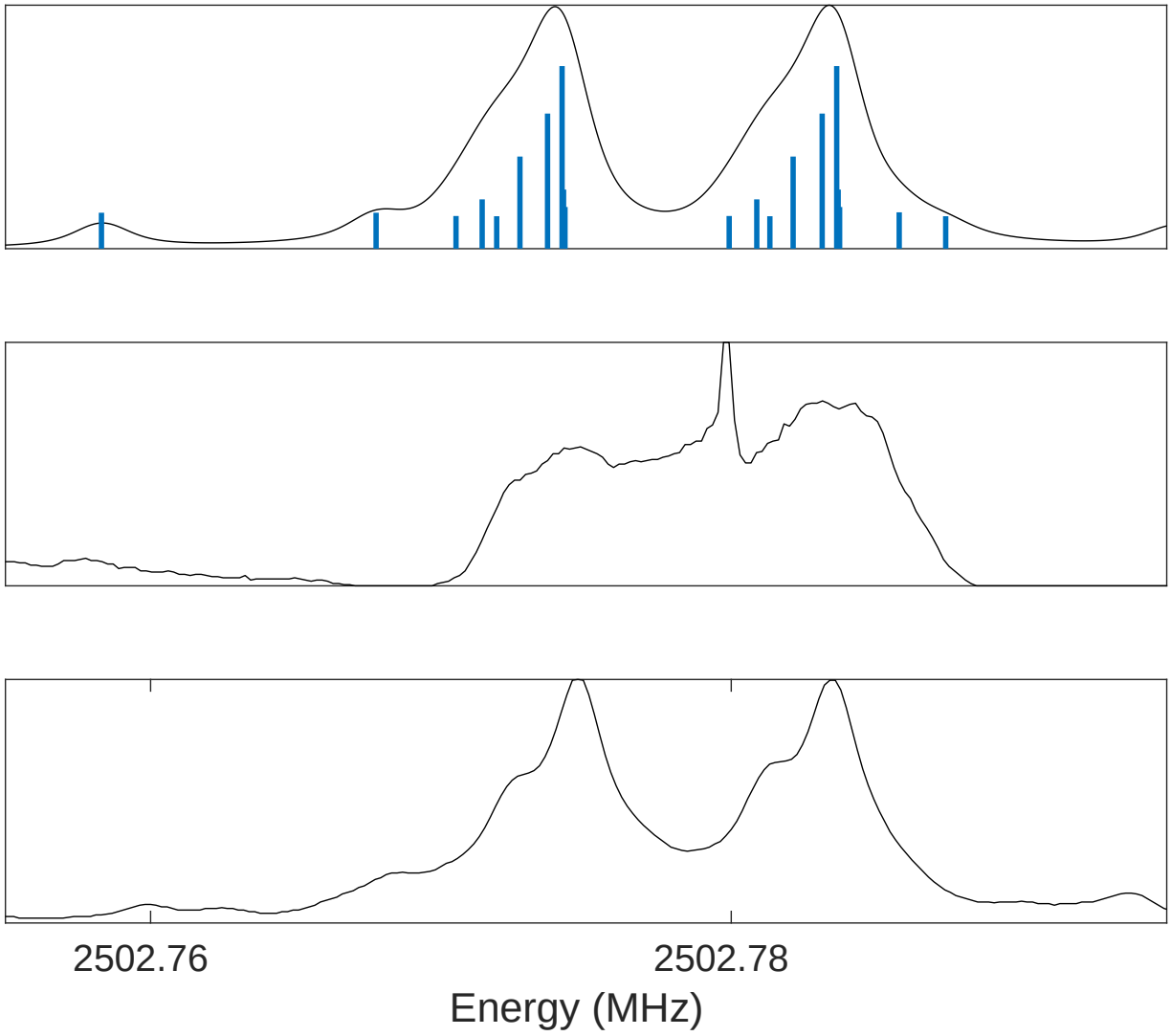

FIG. 1: Comparison of our hyperfine spectrum calculated (upper) for the $2_{11}\ A_2 \leftarrow 2_{12}\ A_1$ transition with the measured spectra (middle)[1] and the fit by Coudert *et al.*[1] (bottom). The Doppler splitting is 9.44 kHz. The blue bars indicate the individual hyperfine transitions with length proportional to the intensity. The hyperfine transitions are convoluted using a Voigt profile with Gaussian width parameter $\sigma = 0.5$ kHz and Lorentz width parameter $\gamma = 0.88$ kHz.

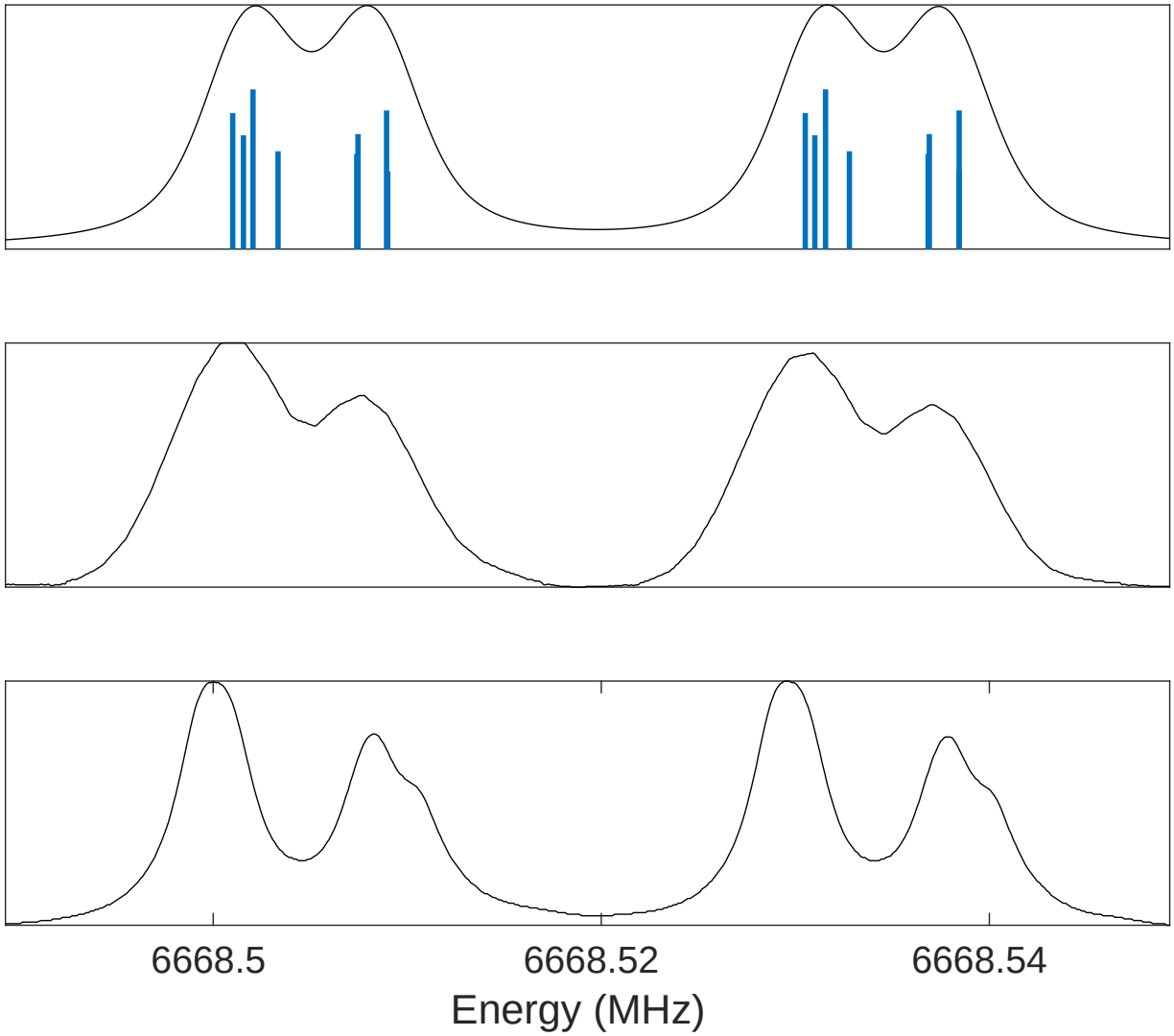

FIG. 2: Comparison of our hyperfine spectrum calculated (upper) for the $5_{15}\ A_2 \leftarrow\ 6_{06} A_1$ transition with the measured spectra (middle) and the fit by Coudert *et al.*[1] (bottom). The Doppler splitting is 29.47 kHz. The blue bars indicate the individual hyperfine transitions with length proportional to the intensity. The hyperfine transitions are convoluted using a Voigt profile with $\sigma = 1.3$ kHz and $\gamma = 1.7$ kHz.

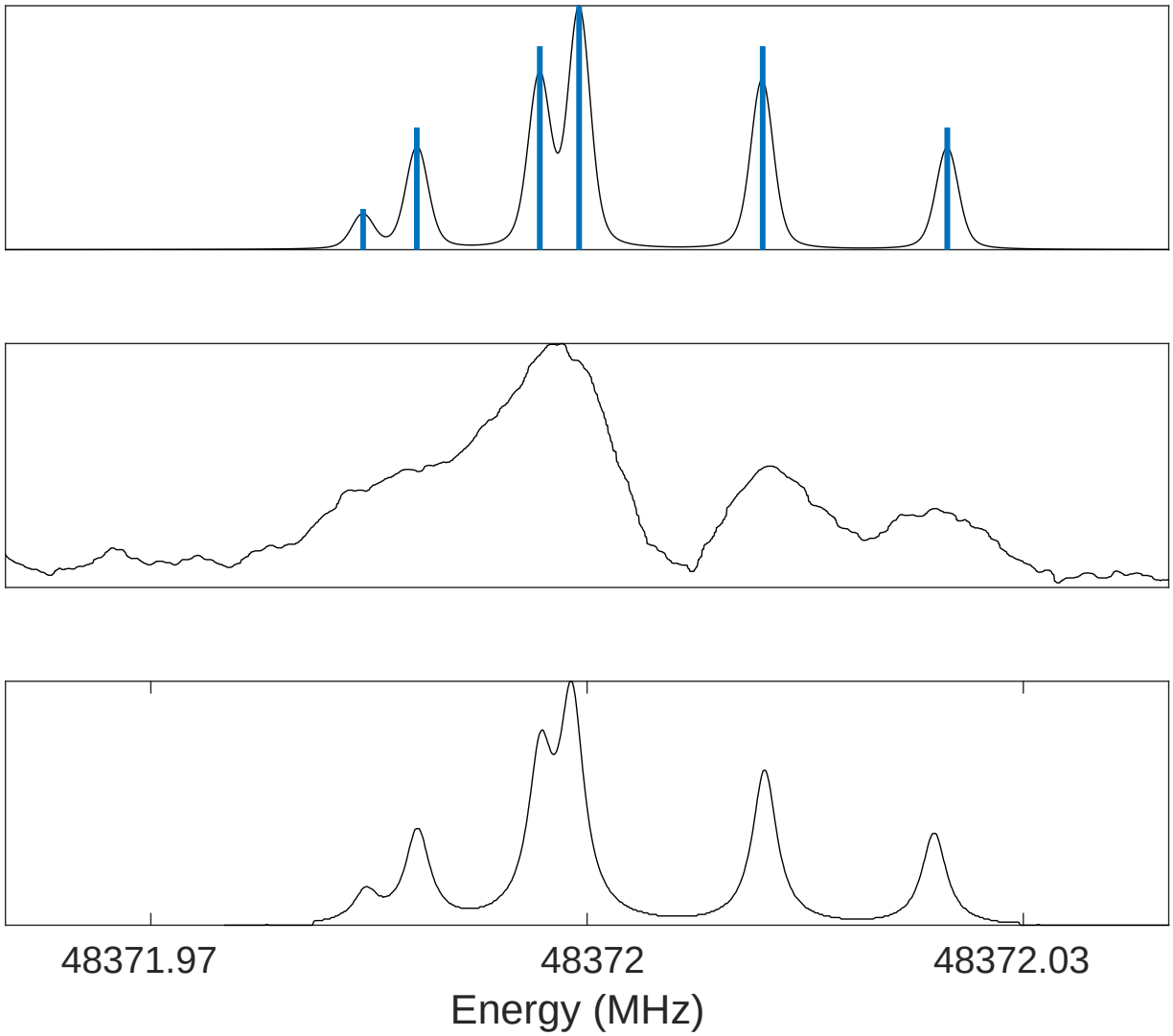

FIG. 3: Comparison of our hyperfine spectrum calculated (upper) for the $1_{01}\ A_2 \leftarrow\ 0_{00}A_1$ transition with the measured spectra (middle)[2] and the fit by Coudert *et al.*[1] (bottom). The blue bars indicate the individual hyperfine transitions with a length proportional to the intensity. The hyperfine transitions are convoluted using a Voigt profile with $\sigma = 0.63$ kHz and $\gamma = 0.3$ kHz.

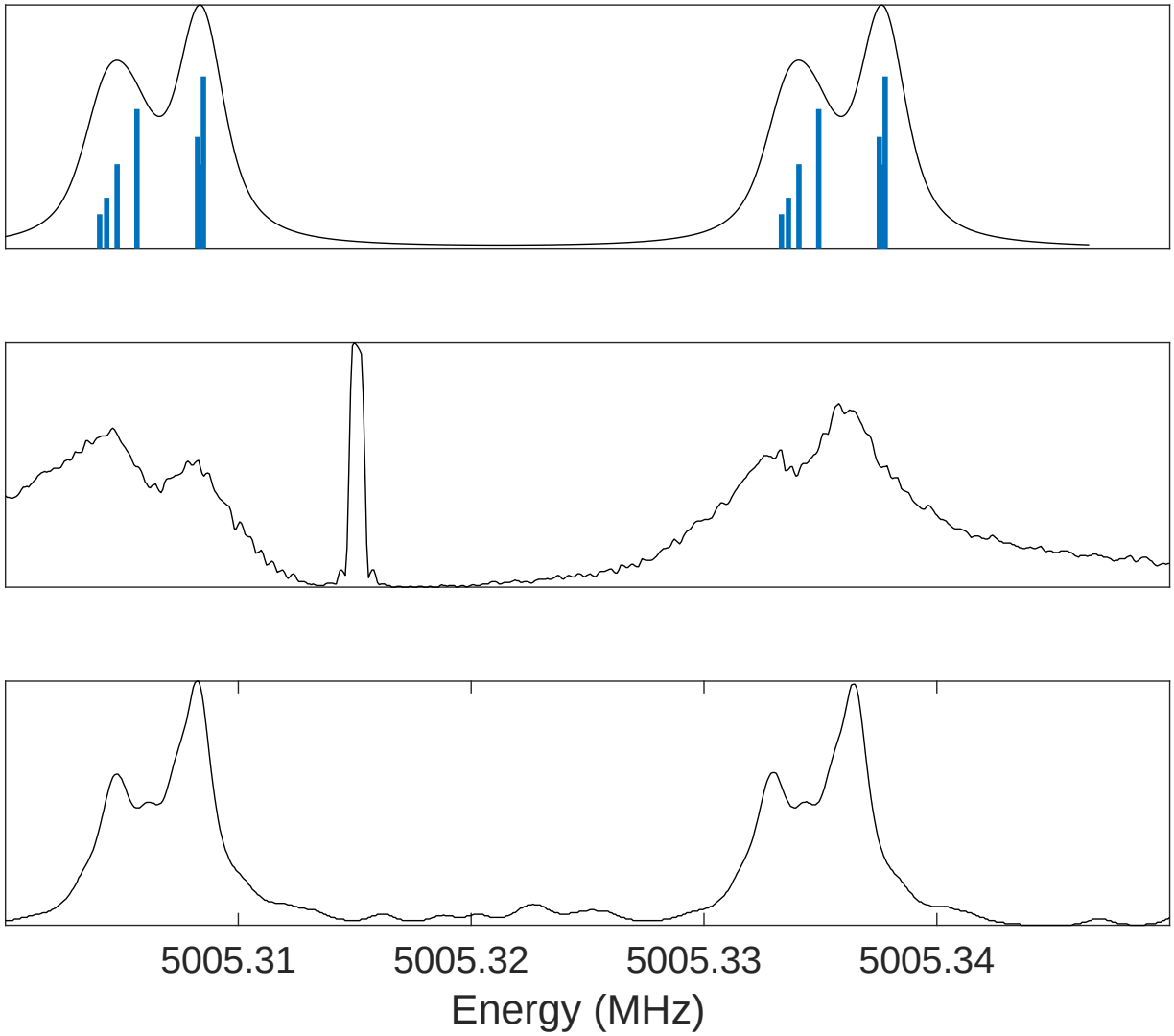

FIG. 4: Comparison of our hyperfine spectrum calculated (upper) for the $3_{12}\ A_2 \leftarrow\ 3_{13}A_1$ transition with the measured spectra (middle)[1] and the fit by Coudert *et al.*[1] (bottom). The Doppler splitting is 29.28 kHz. The blue bars indicate the individual hyperfine transitions with a length proportional to the intensity. The hyperfine transitions are convoluted using a Voigt profile with $\sigma = 0.5$ kHz and $\gamma = 0.88$ kHz.

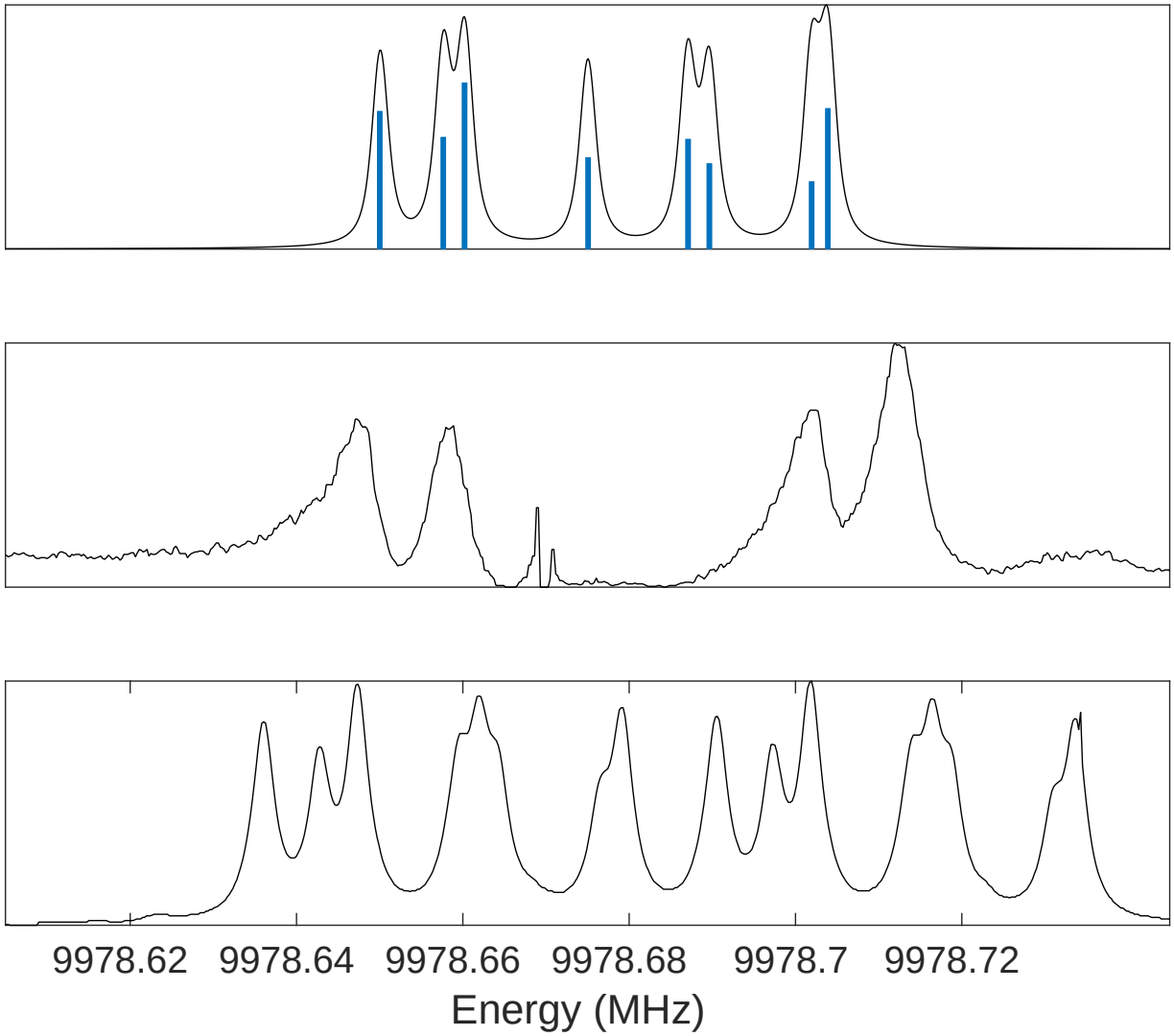

FIG. 5: Comparison of our hyperfine spectrum calculated (upper) for the $4_{32}\ A_2 \leftarrow 5_{23} A_1$ transition with the measured spectra (middle)[1] and the fit by Coudert *et al.*[1] (bottom). No Doppler splitting is used in the calculation. The blue bars indicate the individual hyperfine transitions with a length proportional to the intensity. The hyperfine transitions are convoluted using a Voigt profile with $\sigma = 0.5$ kHz and $\gamma = 0.88$ kHz.

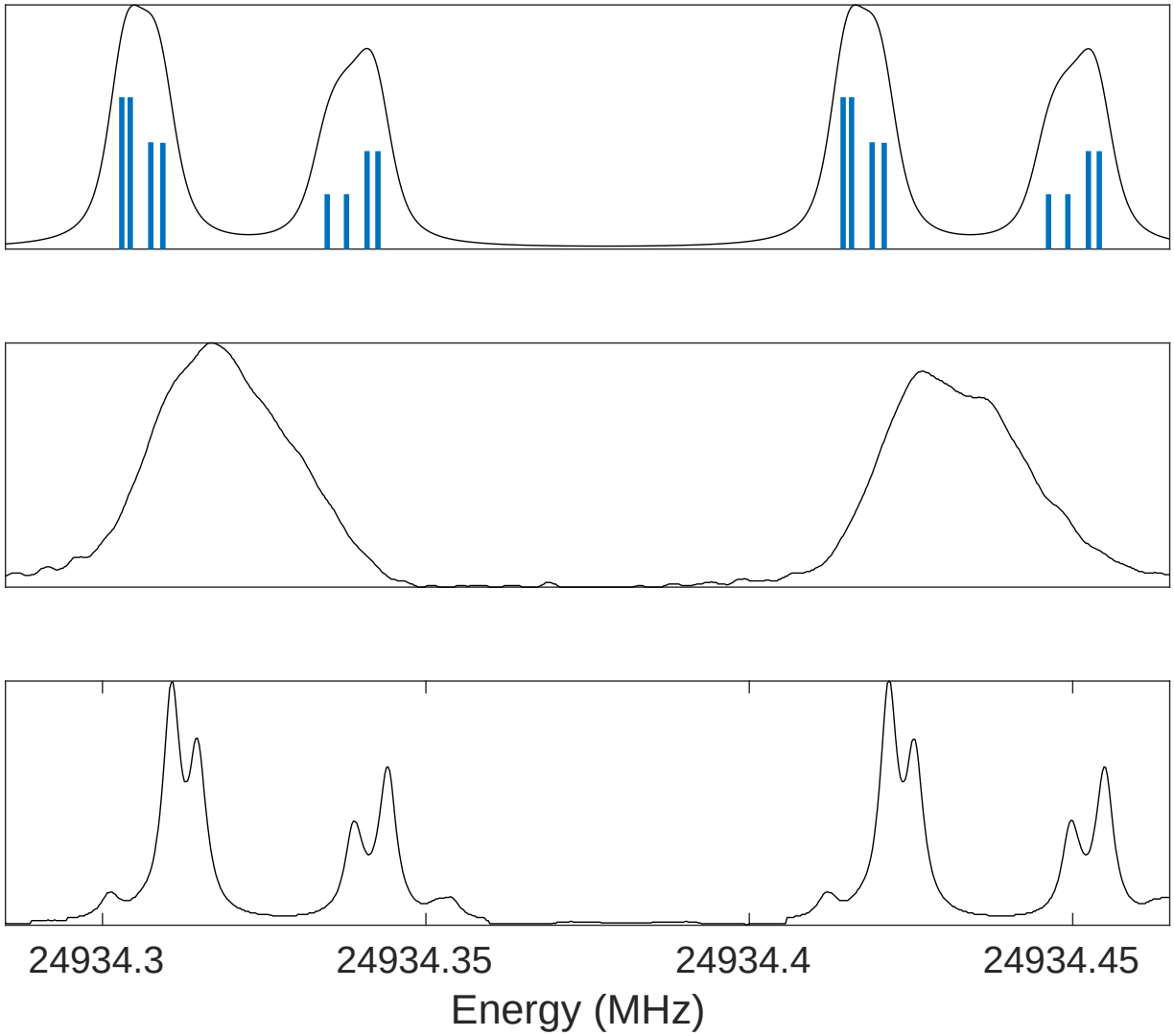

FIG. 6: Comparison of our hyperfine spectrum calculated (upper) for the $2_2\ E \leftarrow\ 2_1 E$ transition with the measured spectra (middle) and the fit by Coudert *et al.*[1] (bottom). The Doppler splitting is 111.52 kHz. The blue bars indicate the individual hyperfine transitions with a length proportional to the intensity. The hyperfine transitions are convoluted using a Voigt profile with $\sigma = 1.5$ kHz and $\gamma = 1.88$ kHz.

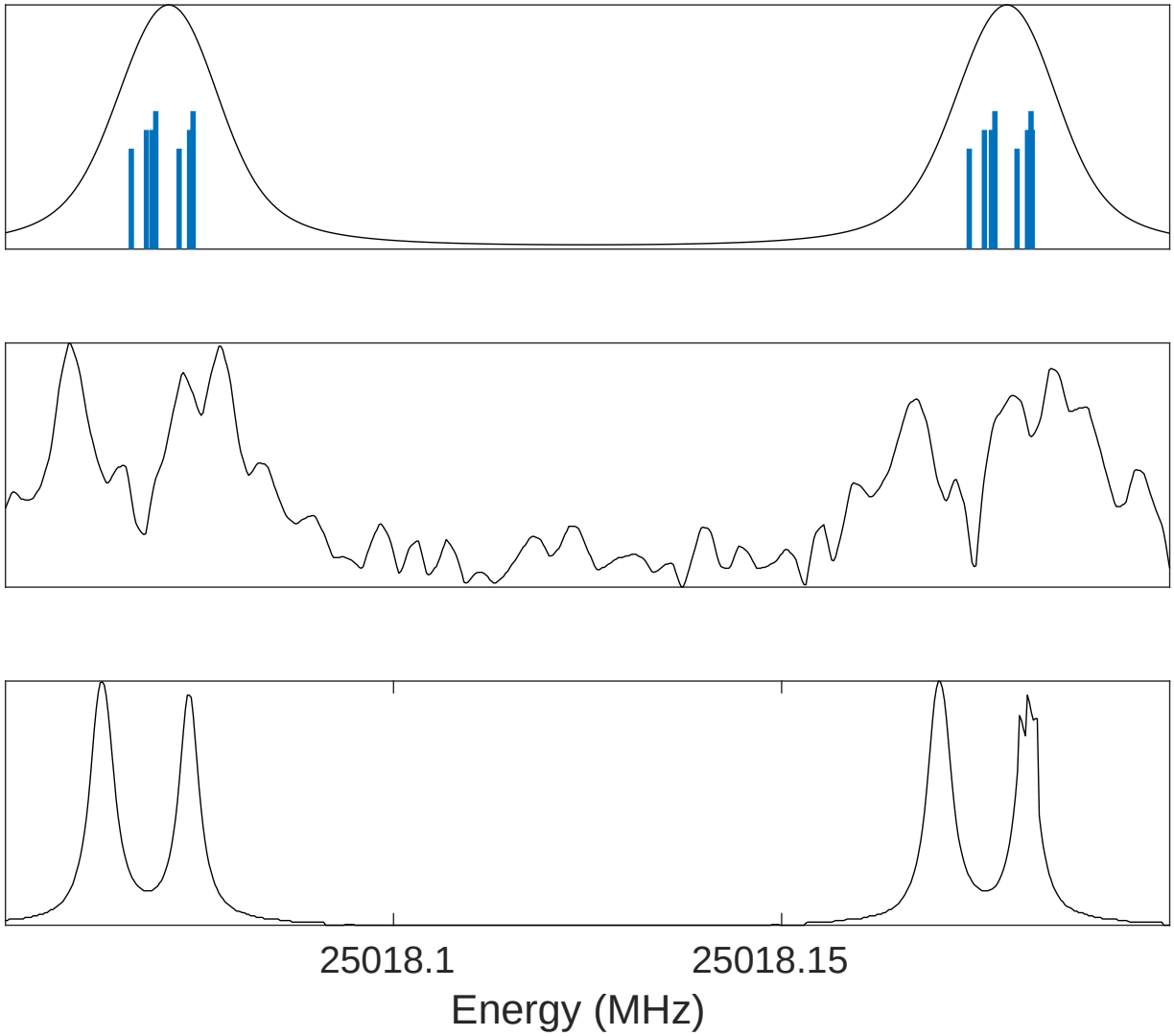

FIG. 7: Comparison of our hyperfine spectrum calculated (upper) for the $6_2\ E \leftarrow\ 6_1 E$ transition with the measured spectra (middle) and the fit by Coudert *et al.*[1] (bottom). The Doppler splitting is 108 kHz. The blue bars indicate the individual hyperfine transitions with a length proportional to the intensity. The hyperfine transitions are convoluted using a Voigt profile with $\sigma = 3.5$ kHz and $\gamma = 3.88$ kHz.

CALCULATED HYPERFINE TRANSITION FREQUENCIES AND INTENSITIES

Tables I to XIV in this supplement list the frequencies and intensities of all allowed hyperfine transitions associated with a given rotational transition. ΔE are the frequency shifts relative to the rotational transition frequency and A are the Einstein coefficients for spontaneous emission. The Einstein B coefficients for absorption and stimulated emission and the transition intensties can be obtained from the A values with the well known relations [3].

TABLE I: Transitions between hyperfine levels with quantum numbers $F_{J_{K_a K_c}}$ within the rotational transition $1_{01}\ A_2 \leftarrow 0_{00}\ A_1$ at 48.373 GHz. Note that the hyperfine splitting vanishes for $J = 0$, so that the $F_{0_{00}} = 1$ and $F_{0_{00}} = 2$ hyperfine levels are degenerate. Therefore, the transition frequency is only determined by the energy of the $F_{1_{01}}$ level. The sum of all Einstein coefficients for transitions with the same frequency from a given $F_{1_{01}}$ level is the same for all $F_{1_{01}}$ levels: $A = 3.817 \cdot 10^{-7}\mathrm{s}^{-1}$.

$F_{1_{01}}$	$F_{0_{00}}$	ΔE (kHz)	A ($10^{-7}\mathrm{s}^{-1}$)
0	1	−18.084	3.817
1	1	−14.350	1.296
1	2	−14.350	2.521
2	1	−5.934	2.891
2	2	−5.934	0.926
3	2	−3.200	3.817
2	1	9.376	0.926
2	2	9.376	2.891
1	1	22.108	2.521
1	2	22.108	1.296

TABLE II: Transitions between hyperfine levels with quantum numbers $F_{J_{K_a K_c}}$ within the rotational transition $2_{11}A_2 \leftarrow 2_{12}\ A_1$ at 2.502 GHz.

$F_{2_{11}}$	$F_{2_{12}}$	ΔE (kHz)	A ($10^{-11}\mathrm{s}^{-1}$)
4	4	1.016	2.205
4	3	−8.122	0.106
4	3	−13.695	0.335
1	1	1.101	1.510
1	2	−4.976	0.833
1	0	−22.115	0.173
1	1	−26.034	0.128
1	2	−26.533	0.002
2	1	7.126	0.494
2	2	1.049	1.285
2	3	−0.563	0.566
2	3	−6.136	0.113
2	1	−20.009	0.122
2	2	−20.508	0.067
3	4	9.628	0.063
3	2	2.102	0.335
3	3	0.489	2.097
3	3	−5.083	0.140
3	2	−19.455	0.010
3	4	14.229	0.504
3	2	6.703	0.147
3	3	5.090	0.007
3	3	−0.482	1.430
3	2	−14.854	0.558
0	1	20.829	0.495
0	1	−6.307	2.152
1	1	24.961	0.145
1	2	18.884	0.186
1	0	1.745	0.709
1	1	−2.174	0.422
1	2	−2.672	1.184
2	1	25.867	0.002
2	2	19.790	0.076
2	3	18.177	0.001
2	3	12.605	0.790
2	1	−1.269	0.705
2	2	−1.767	1.072

TABLE III: Transitions between hyperfine levels with quantum numbers $F_{J_{K_a K_c}}$ within the rotational transition $3_{12}A_1 \leftarrow 3_{13}\ A_2$ at 5.004 GHz.

$F_{3_{12}}$	$F_{3_{13}}$	ΔE (kHz)	A ($10^{-11}\mathrm{s}^{-1}$)
2	2	−2.547	6.260
2	3	−2.806	2.152
2	1	−9.893	1.591
2	3	−19.922	0.531
2	2	−30.210	0.087
3	2	−1.850	1.567
3	3	−2.108	7.386
3	4	−15.535	0.543
3	3	−19.224	0.048
3	4	−21.774	1.078
1	2	4.485	2.604
1	1	−2.860	7.081
1	2	−23.178	0.936
4	3	14.781	0.560
4	4	1.353	7.594
4	3	−2.335	1.194
4	4	−4.885	0.074
4	5	−12.103	1.199
4	3	18.391	0.677
4	4	4.964	0.294
4	3	1.276	0.077
4	4	−1.275	9.475
4	5	−8.492	0.099
3	2	18.857	0.330
3	3	18.599	0.106
3	4	5.171	1.578
3	3	1.483	7.360
3	4	−1.068	0.026
3	2	−8.806	1.222
5	4	15.037	0.887
5	4	8.798	0.175
5	5	1.581	9.559
2	2	29.182	0.143
2	3	28.924	0.003
2	1	21.837	0.533
2	3	11.808	1.681
2	2	1.519	8.262

TABLE IV: Transitions between hyperfine levels with quantum numbers $F_{J_{K_a K_c}}$ within the rotational transition $6_{15}A_2 \leftarrow 6_{16}\ A_1$ at 17.508 GHz.

$F_{6_{15}}$	$F_{6_{16}}$	ΔE (kHz)	A (10^{-11}s^{-1})
8	8	3.318	1.276
8	7	−8.399	0.016
8	7	−13.872	0.031
5	5	2.819	1.244
5	6	−9.616	0.058
5	4	−26.525	0.021
5	5	−34.357	0.000
7	8	8.994	0.017
7	7	−2.723	1.261
7	6	−7.067	0.001
7	7	−8.197	0.003
7	6	−27.153	0.043
6	5	15.271	0.048
6	7	7.179	0.002
6	6	2.836	1.188
6	7	1.706	0.065
6	6	−17.251	0.001
6	5	−21.906	0.020
7	8	20.262	0.037
7	7	8.545	0.000
7	6	4.202	0.055
7	7	3.072	1.223
7	6	−15.884	0.008
4	5	24.807	0.025
4	4	−4.538	1.236
4	5	−12.370	0.064
6	5	29.120	0.000
6	7	21.028	0.049
6	6	16.685	0.007
6	7	15.555	0.006
6	6	−3.401	1.207
6	5	−8.057	0.054
5	5	33.135	0.003
5	6	20.700	0.018
5	4	3.790	0.051
5	6	0.613	0.068
5	5	−4.042	1.184

TABLE V: Transitions between hyperfine levels with quantum numbers $F_{J_{K_a K_c}}$ within the rotational transition $4_{32}A_1 \leftarrow 5_{23}\ A_2$ at 9.977 GHz.

$F_{4_{32}}$	$F_{5_{23}}$	ΔE (kHz)	A (10^{-10}s^{-1})
6	7	−14.760	4.647
6	6	−28.334	0.174
6	5	−29.639	0.003
6	6	−43.699	0.095
6	5	−61.825	0.004
5	4	−20.011	0.005
5	6	−24.931	4.553
5	5	−26.236	0.297
5	6	−40.296	0.001
5	5	−58.422	0.061
5	4	−63.061	0.006
4	4	−11.128	0.276
4	5	−17.352	4.519
4	5	−49.539	0.075
4	3	−50.839	0.005
4	4	−54.178	0.047
3	4	0.046	4.759
3	3	−39.665	0.064
3	4	−43.004	0.099
5	6	44.277	0.001
5	5	42.972	0.001
5	6	28.911	4.646
5	5	10.786	0.267
5	4	6.147	0.006
4	4	50.453	0.003
4	5	44.229	0.035
4	5	12.043	4.440
4	3	10.743	0.010
4	4	7.403	0.434
3	4	57.705	0.052
3	3	17.995	0.429
3	4	14.656	4.441
2	3	26.928	4.922

TABLE VI: Transitions between hyperfine levels with quantum numbers $F_{J_{K_a K_c}}$ within the rotational transition $5_{15}A_2 \leftarrow 6_{06}\ A_1$ at 6.676 GHz.

$F_{5_{15}}$	$F_{6_{06}}$	ΔE (kHz)	A ($\cdot 10^{-9}\mathrm{s}^{-1}$)
7	8	−2.500	1.033
7	7	−6.124	0.014
7	6	−17.228	0.001
7	7	−19.758	0.029
7	6	−31.105	0.000
4	5	−1.240	1.055
4	4	−23.195	0.020
4	5	−32.829	0.002
6	7	4.397	1.035
6	6	−6.707	0.001
6	7	−9.237	0.002
6	6	−20.584	0.038
6	5	−24.151	0.001
5	5	11.130	0.047
5	6	−3.015	1.004
5	4	−10.825	0.001
5	6	−16.892	0.011
5	5	−20.459	0.014
6	5	13.134	0.001
6	7	10.093	0.000
6	6	−1.010	0.055
6	7	−3.541	1.016
6	6	−14.888	0.005
6	5	−18.454	0.001
3	4	4.417	1.077
5	6	16.767	0.006
5	4	8.957	0.001
5	6	2.889	1.015
5	5	−0.677	0.056
4	5	34.424	0.000
4	4	12.469	0.052
4	5	2.835	1.025

TABLE VII: Transitions between hyperfine levels with quantum numbers $F_{J_{K_a}}$ within the rotational transition $2_0 \leftarrow 3_{-1}$ E at 12.178 GHz.

F_{2_0}	$F_{3_{-1}}$	ΔE (kHz)	A (10^{-9}s^{-1})
3	4	4.965	7.372
3	3	3.306	0.293
3	3	−9.120	0.344
3	2	−14.335	0.018
2	3	4.802	7.519
2	3	−7.624	0.221
2	2	−12.839	0.287
2	3	7.667	0.098
2	3	−4.760	7.325
2	2	−9.974	0.605
1	2	−7.978	8.027
2	3	1.475	5.711
2	3	−11.352	1.495
2	2	−17.669	0.821
3	4	6.106	7.372
3	3	5.844	0.325
3	3	−6.982	0.312
3	2	−13.300	0.018
2	3	6.980	1.861
2	3	−5.847	6.095
2	2	−12.164	0.071
1	2	−3.263	8.027

TABLE VIII: Transitions between hyperfine levels with quantum numbers $F_{J_{K_a}}$ within the rotational transition $2_1 \leftarrow 3_0$ E at 19.969 GHz.

F_{2_1}	F_{3_0}	ΔE (kHz)	A ($\cdot 10^{-8}\mathrm{s}^{-1}$)
2	3	−2.620	0.968
2	3	−8.871	0.320
2	2	−17.451	0.063
3	3	−2.433	0.093
3	4	−6.237	1.241
3	3	−8.685	0.014
3	2	−17.265	0.003
2	3	16.433	0.253
2	3	10.182	1.012
2	2	1.601	0.087
1	2	4.050	1.352
3	4	−5.490	1.241
3	3	−7.651	0.040
3	3	−11.639	0.067
3	2	−14.276	0.003
2	3	−4.782	1.291
2	3	−8.769	0.000
2	2	−11.407	0.061
2	3	10.700	0.005
2	3	6.713	1.258
2	2	4.075	0.089
1	2	11.265	1.352

TABLE IX: Transitions between hyperfine levels with quantum numbers $F_{J_{K_a}}$ within the rotational transition $2_2 \leftarrow 2_1$ E at 24.935 GHz.

F_{2_2}	F_{2_1}	ΔE (kHz)	A (10^{-8}s^{-1})
3	2	−16.061	0.188
3	3	−16.247	3.553
3	2	−35.113	0.256
2	2	−9.941	3.480
2	3	−10.128	0.221
2	2	−28.994	0.083
2	1	−31.443	0.213
1	2	39.917	0.422
1	2	20.865	0.577
1	1	18.416	2.998
2	2	40.690	0.001
2	3	40.504	0.401
2	2	21.638	3.209
2	1	19.189	0.386
3	3	−14.961	3.553
3	2	−17.831	0.180
3	2	−33.313	0.264
2	3	−8.881	0.221
2	2	−11.751	3.498
2	2	−27.233	0.065
2	1	−34.422	0.213
1	2	38.099	0.404
1	2	22.617	0.595
1	1	15.427	2.998
2	3	41.792	0.401
2	2	38.922	0.005
2	2	23.440	3.205
2	1	16.251	0.386

TABLE X: Transitions between hyperfine levels with quantum numbers $F_{J_{K_a}}$ within the rotational transition $3_2 \leftarrow 3_1$ E at 24.933 GHz.

F_{3_2}	F_{3_1}	ΔE (kHz)	A (10^{-8}s^{-1})
4	4	−8.336	4.699
4	3	−12.007	0.145
4	3	−25.336	0.168
3	4	−4.694	0.167
3	3	−8.365	4.641
3	3	−21.694	0.041
3	2	−30.970	0.165
3	4	30.502	0.236
3	3	26.831	0.000
3	3	13.502	4.543
3	2	4.226	0.233
2	3	30.418	0.259
2	3	17.089	0.298
2	2	7.813	4.456
4	3	−9.491	0.149
4	4	−10.388	4.699
4	3	−27.937	0.164
3	3	−5.704	4.630
3	4	−6.601	0.166
3	3	−24.150	0.052
3	2	−27.369	0.164
3	3	29.339	0.002
3	4	28.442	0.236
3	3	10.893	4.541
3	2	7.674	0.234
2	3	33.099	0.265
2	3	14.653	0.292
2	2	11.434	4.456

TABLE XI: Transitions between hyperfine levels with quantum numbers $F_{J_{K_a}}$ within the rotational transition $4_2 \leftarrow 4_1$ E at 24.944 GHz.

F_{4_2}	F_{4_1}	ΔE (kHz)	A (10^{-8}s^{-1})
5	4	−5.333	0.109
5	5	−6.560	5.266
5	4	−24.872	0.110
4	4	−2.449	5.216
4	5	−3.676	0.121
4	4	−21.988	0.028
4	3	−25.454	0.120
4	4	24.596	0.003
4	5	23.370	0.147
4	4	5.058	5.189
4	3	1.592	0.147
3	4	29.960	0.171
3	4	10.421	0.172
3	3	6.955	5.142
5	5	−3.679	5.266
5	4	−8.540	0.108
5	4	−21.455	0.111
4	5	−1.135	0.121
4	4	−5.997	5.220
4	4	−18.911	0.024
4	3	−29.806	0.120
4	5	26.272	0.147
4	4	21.411	0.001
4	4	8.496	5.190
4	3	−2.399	0.146
3	4	26.376	0.169
3	4	13.462	0.174
3	3	2.567	5.142

TABLE XII: Transitions between hyperfine levels with quantum numbers $F_{J_{K_a}}$ within the rotational transition $5_2 \leftarrow 5_1$ E at 24.978 GHz.

F_{5_2}	F_{5_1}	ΔE (kHz)	A (10^{-8}s^{-1})
6	6	0.026	5.570
6	5	−6.199	0.081
6	5	−19.387	0.078
5	6	2.002	0.090
5	5	−4.223	5.538
5	5	−17.411	0.012
5	4	−29.834	0.090
5	6	24.801	0.098
5	5	18.577	0.001
5	5	5.388	5.533
5	4	−7.034	0.098
4	5	24.149	0.116
4	5	10.961	0.113
4	4	−1.462	5.500
6	5	−2.355	0.081
6	6	−3.754	5.570
6	5	−23.664	0.078
5	5	0.271	5.537
5	6	−1.129	0.090
5	5	−21.038	0.013
5	4	−24.648	0.090
5	5	22.379	0.001
5	6	20.979	0.098
5	5	1.070	5.532
5	4	−2.540	0.098
4	5	28.703	0.117
4	5	7.394	0.113
4	4	3.784	5.500

TABLE XIII: Transitions between hyperfine levels with quantum numbers $F_{J_{K_a}}$ within the rotational transition $6_2 \leftarrow 6_1$ E at 25.046 GHz.

F_{6_2}	F_{6_1}	ΔE (kHz)	A (10^{-8}s^{-1})
7	6	−0.060	0.063
7	7	−1.562	5.887
7	6	−23.467	0.060
6	6	2.674	5.865
6	7	1.172	0.071
6	6	−20.733	0.004
6	5	−24.459	0.071
6	7	19.871	0.071
6	6	−2.035	5.869
6	5	−5.761	0.071
5	6	28.507	0.086
5	6	5.101	0.081
5	5	1.375	5.843
7	7	3.193	5.887
7	6	−4.482	0.063
7	6	−18.274	0.060
6	7	4.835	0.071
6	6	−2.840	5.865
6	6	−16.632	0.004
6	5	−30.555	0.071
6	7	24.699	0.071
6	6	3.232	5.869
6	5	−10.691	0.071
5	6	22.898	0.086
5	6	9.105	0.081
5	5	−4.817	5.843

TABLE XIV: Transitions between hyperfine levels with quantum numbers $F_{J_{K_a}}$ within the rotational transition $9_{-1} \leftarrow 8_{-2}$ E at 9.909 GHz.

$F_{9_{-1}}$	$F_{8_{-2}}$	ΔE (kHz)	A ($10^{-9}\mathrm{s}^{-1}$)
10	9	3.418	1.131
9	9	7.901	0.008
9	8	3.528	1.122
9	8	−18.877	0.001
9	9	22.435	0.006
9	8	18.063	0.001
9	8	−4.343	1.123
8	9	32.129	0.000
8	8	27.757	0.008
8	8	5.351	0.008
8	7	−3.809	1.115
10	9	4.433	1.131
9	9	7.140	0.008
9	8	2.360	1.121
9	8	−19.406	0.002
9	9	22.867	0.006
9	8	18.087	0.003
9	8	−3.679	1.122
8	9	32.119	0.000
8	8	27.339	0.008
8	8	5.573	0.008
8	7	−4.509	1.115

[1] L. Coudert, C. Gutlé, T. Huet, J.-U. Grabow, and S. Levshakov, "Spin-torsion effects in the hyperfine structure of methanol," *J. Chem. Phys.*, vol. 143, no. 4, p. 044304, 2015.

[2] J. E. M. Heuvel, *Hyperfine structure in internal rotor molecules.* PhD thesis, Katholieke Universiteit Nijmegen, 1972.

[3] R. C. Hilborn, "Einstein coefficients, cross sections, f values, dipole moments and all that," *Am. J. Phys.*, vol. 50, pp. 982–986, 1982.